Geophysica (1989), **25**, 1&2, 21–35

A Stability Investigation of a Three Level Quasi-Geostrophic Model

A. Wiin-Nielsen

Geophysical Institute & University of Copenhagen

Abstract

This paper contains an analysis of the stability properties of a three level quasi-geostrophic model and a determination of the structure of the growing baroclinic waves. The model is the minimum model which permits deviations from a linear vertical windprofile and a vertical variation of the static stability parameter. In spite of the numerous investigations of baroclinic, quasi-geostrophic models, which can be found in the meteorological literature over the last forty years, it appears that this minimum model has not been analysed.

Contrary to the two-level model the three-level model contains for certain wind distributions the instability for very long waves in addition to the normal instability for Rossby waves. The two-level model predicts that unstable baroclinic waves will have a westward slope with height and thus transport heat to the north. This is not necessarily true for all unstable waves in the three-level model.

A third strongly unstable region for very short waves appears if one of the layers become nearly adiabatic. This mesoscale instability may be connected with the precursor, necessary for the formation of polar lows.

The additional degrees of freedom in the three-level model permits an investigation of the stability for simple variations of the static stability parameters as well as the stability of low level baroclinic zones. Such results will be reported together with the structure of the growing baroclinic waves.

1. *Introduction*

The classical study of atmospheric baroclinic stability was made by *Charney* (1947). He considered a basic state characterized by a linearly increasing westerly current and a constant lapse-rate in the temperature field and found that amplifying baroclinic waves should exist for sufficiently large vertical windshear. Similar results were obtained by *Eady* (1949). Numerous studies have since then been made of the two-level model. Well known investigations are those of *Eliassen* (1952) and *Phillips* (1954).

The three-level model has been investigated by *Cressman* (1961) and *Wiin-Nielsen* (1961) but these studies did not include a stability investigation. Studies which were

quite different from Charney's analytical approach were conducted by *Green* (1960) who solved the baroclinic stability problem using numerical methods. An instability for very long waves were found in these numerical studies which of course permitted more general basic states than those which could be treated in the purely mathematical approach. Another numerical study of the baroclinic problem was made by *Haltiner* (1963). An attempt to investigate more realistic vertical profiles of the horizontal wind in the basic state were made by *Wiin-Nielsen* (1967), but due to mathematical difficulties it was necessary to use an adiabatic stratification in the basic state.

In the present study we shall employ the standard three-level, quasi-geostrophic model, which permits simple deviations from the linear profile of the horizontal wind and an elementary vertical variation of the stability parameter. As expected the frequency equation is an algebraic equation of the third degree. The equation is solved using the classical formulas, but it is advantageous to do all calculations numerically due to the rather complicated nature of the coefficients. The solution of the eigenvalue problem will be followed by a determination of the structure of the growing baroclinic wave.

The present study of the three-level model came as a byproduct of an investigation of baroclinic instability as a precursor for the formation of the small, but intense polar lows (*Wiin-Nielsen*, 1989). This problem is one of investigating whether or not a baroclinic instability can occur on a rather small scale, say less than 1000 km. As it turns out, such an instability is found in the three-level model if the stratification of the lower layer is nearly adiabatic, a situation which is characteristic of the airmass in which polar lows are formed. In the polar low study the beta-effect may be neglected, but if this effect is reintroduced one may consider the larger scales as well as is done in this paper. The main reason to record this three-level stability study is that such a model is the simplest model which can produce instability on the small as well as the very large scale.

2. *The model equations*

The standard model used here applies the vorticity equation in its quasi-geotrophic form at the pressure levels $p_0/6$, $3p_0/6$ and $5p_0/6$ where $p_0 = 100\,\text{kPa}$. Quantities at these levels are denoted by subscripts 1, 3 and 5, respectively. This means that the streamfunction and the relative vorticity are measured at these levels. According to the structure of the quasi-geostrophic vorticity equation this implies that the vertical p-velocity should be measured at levels 0, $p_0/3$, $2p_0/3$ and p_0, indicated by the subscripts 0, 2, 4 and 6. The simplified boundary conditions will be $w_0 = w_6 = 0$. Internally, its vertical column has two vertical velocities w_2 and w_4. To eliminate the vertical velocity from the equations one applies the thermodynamic equation in the adiabatic

form at levels 2 and 4. It is then convenient to introduce two thermal streamfunctions

$$\begin{aligned} \psi_T &= \psi_1 - \psi_3, \\ \psi_B &= \psi_3 - \psi_5 \end{aligned} \tag{2.1}$$

with corresponding relations for the vorticity, ζ.

The stability parameters are denoted σ_2 and σ_4 where in general

$$\sigma = -\alpha \frac{\partial \ln \Theta}{\partial p} \tag{2.2}$$

The factors containing the static stability are denoted:

$$q_2^2 = \frac{f_0^2}{\sigma_2 P^2}\,; \qquad q_2^2 = \frac{f_0^2}{\sigma_4 P^2}\,; \qquad P = \frac{1}{3} \cdot 100\,\mathrm{kPA}, \qquad f_0 = 10^{-4}\mathrm{s}^{-1} \tag{2.3}$$

After elimination of w_2 and w_4 one obtains the equations:

$$\begin{aligned} &\frac{\partial}{\partial t}\left[\zeta_3 - q_4^2\psi_B + q_2^2\psi_T\right] + \vec{V}_3 \cdot \nabla\left[\zeta_3 - q_4^2\psi_B + q_2^2\psi_T\right] + \beta v_3 = 0 \\ &\frac{\partial}{\partial t}\left[\zeta_T - 2q_2^2\psi_T + q_4^2\psi_B\right] + \vec{V}_3 \cdot \nabla\left[\zeta_T - 2q_2^2\psi_T + q_4^2\psi_B\right] + \vec{V}_T \cdot \nabla(\zeta_3 + \zeta_T) + \beta v_T = 0 \\ &\frac{\partial}{\partial t}\left[\zeta_B - 2q_4^2\psi_B + q_2^2\psi_T\right] + \vec{V}_3 \cdot \nabla\left[\zeta_B - 2q_4^2\psi_T + q_2^2\psi_B\right] + \vec{V}_B \cdot \nabla(\zeta_3 - \zeta_B) + \beta v_B = 0 \end{aligned} \tag{2.4}$$

where $\beta = df/dy$ is the Rossby parameter.

The basic state will be given by the zonal velocities U_3, U_T and U_B implying that $U_1 = U_3 + U_T$ and $U_5 = U_3 - U_B$. In addition, one must specify σ_2 and σ_4. This could of course be done by two numbers taken from climatology, but we shall prefer to say that the layers from levels 5 to 3, and from 3 to 1 are characterized by constant lapse rates, denoted by η_B and η_T. According to *Jacobs and Wiin-Nielsen* (1966) we find the stability factor σ for a constant lapse rate atmosphere from the formula

$$\sigma = \frac{R^2 T_0}{g p_0^2}(\eta_d - \eta) p_*^{-(2 - \frac{R\eta}{g})}\,; \qquad p_* = \frac{p}{p_0} \tag{2.5}$$

Adapting (2.5) to the two layers described above we find

$$\sigma_4 = \frac{R^2 T_0}{g p_0^2}(\eta_d - \eta_B) p_{*_4}^{-(2 - \frac{R\eta_B}{g})} \tag{2.6}$$

and

$$\sigma_2 = \frac{R^2 T_0}{g p_0^2}(\eta_d - \eta_T) p_{*3}^{\frac{R}{g}(\eta_B - \eta_T)} p_{*2}^{-(2 - \frac{R\eta_T}{g})} \tag{2.7}$$

in which $R = 287\,\mathrm{Jkg^{-1}K^{-1}}$, $T_0 = 283\,\mathrm{K}$, $g = 9.8\,\mathrm{ms^{-2}}$ and $\eta_d = g/C_p$, $C_p = 1004\,\mathrm{Jkg^{-1}K^{-1}}$. If $\eta_B = \eta_T = 6.5 \cdot 10^{-3}\mathrm{Km^{-1}}$ we find $\sigma_4 = 1.73$ and $\sigma_2 = 6.08$ (in SI-units).

On the steady state defined above we superimpose perturbations of the form

$$(\psi_3, \psi_T, \psi_B) = (\hat{\psi}_3, \hat{\psi}_T, \hat{\psi}_B) \exp[ik(x - ct)] \tag{2.8}$$

The expressions for the perturbations (2.8) are substituted in the equations (2.4) which are linearized at the same time. The procedure leads to three linear homogeneous equations which will have a non-trivial solution if the determinant of the coefficient matrix has the value zero. The equations may be written in the form

$$\begin{bmatrix} \lambda_2^2 U_T - \lambda_4^2 U_B - C_R - y & \lambda_2^2 y & -\lambda_4^2 y \\ (1 - 2\lambda_2^2) U_T + \lambda_4^2 U_B & U_T - (1 + 2\lambda_2^2) y - C_R & \lambda_4^2 y \\ (1 - 2\lambda_4^2) U_B + \lambda_2^2 U_T & \lambda_2^2 y & -U_B - (1 + 2\lambda_4^2) x - C_R \end{bmatrix} \begin{bmatrix} \hat{\psi}_3 \\ \hat{\psi}_T \\ \hat{\psi}_B \end{bmatrix} = 0 \tag{2.9}$$

in which we have introduced the notations:

$$\lambda_2^2 = q_2^2/k^2; \qquad \lambda_4^2 = q_4^2/k^2; \qquad y = c - U_3, \qquad C_R = \beta/k^2 \tag{2.10}$$

The determinant in (2.9) may be evaluated in the usual way resulting in the following equation

$$a_3 y^3 + a_2 y^2 + a_1 y + a_0 = 0 \tag{2.11}$$

where

$$\begin{aligned} a_3 &= 1 + 2\lambda_2^2 + 2\lambda_4^2 + 3\lambda_2^2\lambda_4^2 \\ a_2 &= (1 + 2\lambda_2^2 + 2\lambda_4^2 + 2\lambda_2^2\lambda_4^2)(U_B - U_T) + C_R[3(1 + \lambda_2^2\lambda_4^2) + 4(\lambda_2^2 + \lambda_4^2)] \\ a_1 &= \lambda_4^2(1 + \lambda_2^2) U_B^2 + \lambda_2^2(1 + \lambda_4^2) U_T^2 - (1 + 2\lambda_2^2 + 2\lambda_4^2) U_B U_T + \\ &\quad (3 + 2\lambda_2^2 + 2\lambda_4^2) C_R^2 + (2 + 2\lambda_2^2 + 2\lambda_4^2 + \lambda_2^2\lambda_4^2) C_R(U_B - U_T) + C_R(\lambda_4^2 U_B - \lambda_2^2 U_T) \\ a_0 &= U_B U_T(\lambda_2^2 U_T - \lambda_4^2 U_B) + C_R^3 + (1 + \lambda_4^2) C_R^2 U_B - (1 + \lambda_2^2) C_R^2 U_T \\ &\quad - (1 + \lambda_2^2 + \lambda_4^2) C_R U_B U_T + C_R(\lambda_2^2 U_T^2 + \lambda_4^2 U_B^2) \end{aligned} \tag{2.12}$$

Equation (2.11) is solved using the classical formulas for the roots of which one is real and the other two may be real or form a pair of complex, conjugate numbers.

When the values of $y = c - U_3$ are known we can go back to the system (2.9), use any two of the equations and calculate the relative amplitudes and phases for the unstable (or the stable) wave. In the following section we shall discuss the results.

3. *Results and discussion*

The procedures established in section 2 suffice to determine the stability as a function of the wavelength, the two windshears and the two values of the static stability.

In the first example we select $U_B = U_T = U_s$ and $\eta_B = \eta_T = 6.5 \cdot 10^{-3}\mathrm{Km}^{-1}$ while η_d is set to $10^{-2}\mathrm{Km}^{-1}$. Equation (2.11) was solved in each point of a grid in the (L,U_s) plane. The wavelength was varied in steps of $5 \cdot 10^5$ m and the windshear in steps of $5\,\mathrm{ms}^{-1}$. This case differs from a two-level model only in the vertical variation of the static stability parameter. For each value of U_s it turns out that instability occurs in two intervals of the wavelength. Based on these calculations Fig. 1 was prepared showing the two regions of instability, marked I. The boundaries of the regions of instability are

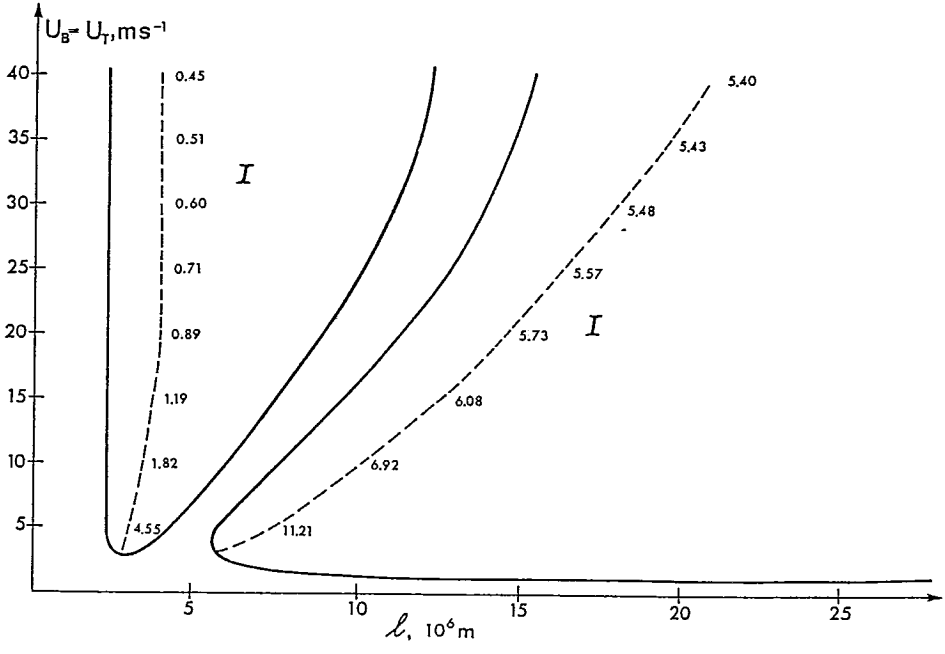

Fig. 1. The regions of instability, marked I, in a diagram with wavelength as abscissa and windshear as ordinate. In this case $U_B = U_T$. The dashed lines indicate maximum instability, and the numbers give the e-folding time in days.

drawn on the basis of the numerical calculations in the grid points and are therefore accurate only to the size between the grid points. It is nevertheless certain that the two regions of instability exist as separate regions. The numerical results permit also an approximate determination of the two curves of maximum instability given as dashed lines in Fig. 1. Along these lines the e-folding time, measured in days, are given.

The region of instability for the shorter waves is very similar to the corresponding region of instability found in a two-level model including e-folding times of the order of 1 day for realistic values of U_s. The second region of instability for the longer waves is not found in a two-level model. It has a much smaller degree of instability since even the smallest e-folding times are larger than 5 days.

To explore the difference between the two regions of instability the amplitude ratios $a_1 = A_1/A_3$ and $a_5 = A_5/A_3$ were calculated. They are obtained from the linear homogeneous system (2.9) where $y = c - U_3$ has been obtained from the solution of (2.11). Using two of the three equations we may calculate $\hat{\psi}_T/\hat{\psi}_3$ and $\hat{\psi}_B/\hat{\psi}_3$, and from these complex values we may then determine not only the relative amplitude, but also the relative phase angles for the amplifying waves. Fig. 2 shows the relative amplitudes and Fig. 3 the relative phase angles $\delta_1 = \Theta_1 - \Theta_3$ and $\delta_5 = \Theta_5 - \Theta_3$ where

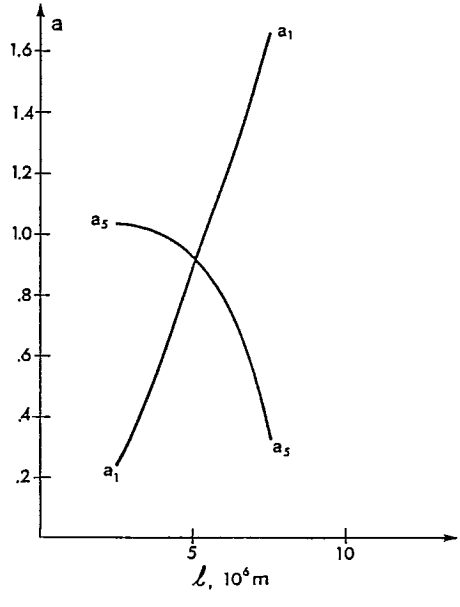

Fig. 2. The relative amplitudes at levels 1 and 5 as a function of wavelength for short waves. $U_B = U_T = 15\ \mathrm{ms}^{-1}$, $\eta_B = \eta_T = 6.5 \cdot 10^{-3}\mathrm{Km}^{-1}$

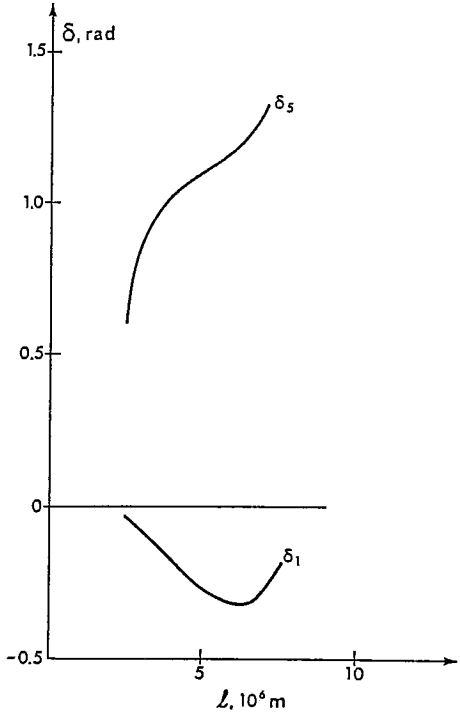

Fig. 3. The relative phases at levels 1 and 5 as a function of wavelength. Parameters as in Fig. 2.

the phase angle is determined as the position of the ridge in the wave. From Fig. 3 we observe that these amplifying waves slope westward with height with a larger slope in the lower than in the upper part of the atmosphere. Fig. 2 shows that for the specific values selected here $a_5 > a_1$, for the shorter waves while the opposite is true for the longer waves in this region. Both the smaller slope δ_1, and the small value of a_1 for the shorter waves are due to the larger value of the stability parameter in the upper part of the model. It is known that the static stability parameter dominates for short waves resulting in stability for the shortest waves (in this case $L < 2.5 \cdot 10^6$ m).

Next, we turn our interest to the weak instability for the longest waves. Fig. 4 which shows the relative amplitudes indicates not only that $a_1 > a_5$ for all wavelengths, but more importantly that both a_1 and a_5 are larger than 1. This means that the smallest amplitude is in the middle of the atmosphere with larger amplitudes above and below. The slowly growing long waves belong therefore to a class involving the higher baroclinic modes which are possible in a three-level, but not in a two-level model. The instability for these long waves was apparently first found by *Green* (1960) who made

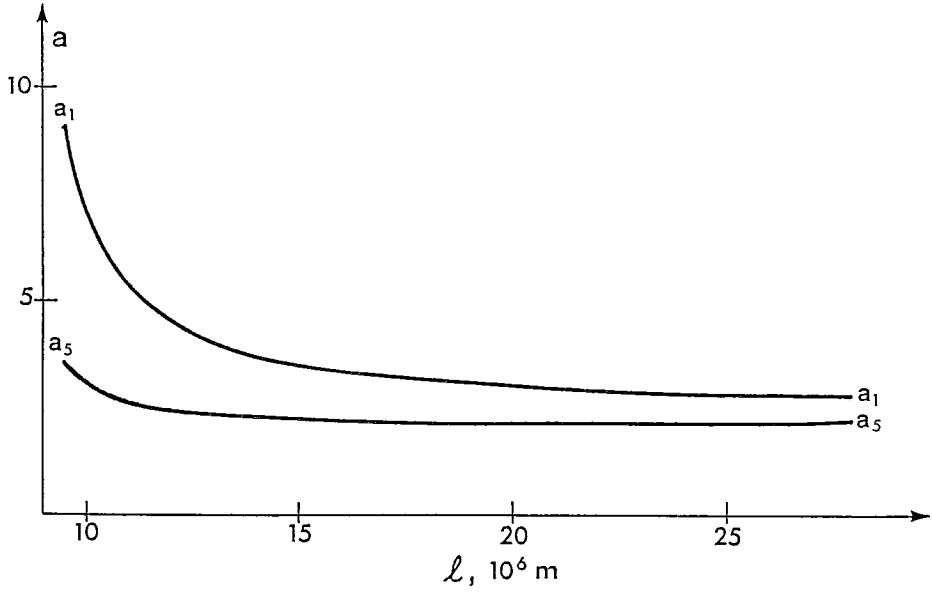

Fig. 4. The relative amplitudes at levels 1 and 5 as a function of wavelength for long waves. Parameters as in Fig. 2.

a numerical determination of the eigenvalues in a multi-level, quasi-geostrophic model, developed originally by *Eady* (1949) for the continuous case. In the present case of the three-level model the weak long wave instability is connected with the vertical variation of the static stability parameter. This can easily be seen by replacing both σ_2 and σ_4 by the same value, say $\frac{1}{2} \cdot (\sigma_2 + \sigma_4)$. A recalculation of the stability diagram as shown in Fig. 1 indicates that the long wave instability disappears, and the result is that of a pure two-level model.

Next we turn to the vertical slope of the very long unstable waves. Fig. 5 shows in a form analogous to Fig. 3 the phase differences δ_1 and δ_5. Also in this case we find a westward sloping wave since $\delta_5 > 0$ and $\delta_1 < 0$, but the difference $\delta_5 - \delta_1$ is in this case so large that it represents slightly more than half a wavelength. Approximately, a low at the low level 5 will have a high at the upper level 1.

The following calculations were made with $U_B = 15\,\mathrm{ms}^{-1}$ and $\eta_B = \eta_T = 6.5 \cdot 10^{-3}\mathrm{Km}^{-1}$. U_T was varied from $-30\,\mathrm{ms}^{-1}$ to $30\,\mathrm{ms}^{-1}$ in intervals $5\,\mathrm{ms}^{-1}$. The computations were made in a grid in the (L, U_T)-plane and on the basis of the results Fig. 6 was drawn. The regions marked S are regions of stability. They consist of three parts: the short waves for all values of U_T, an intermediate group which is stable for $U_T > -5\,\mathrm{ms}^{-1}$, and a group of long waves which are stable when $U_T < -10\,\mathrm{ms}^{-1}$

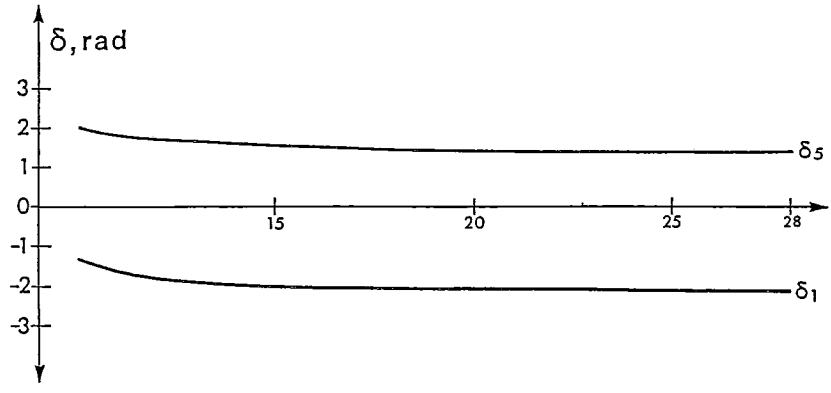

Fig. 5. The relative phases at levels 1 and 5 as a function of wavelength for long waves. Parameters as in Fig. 2.

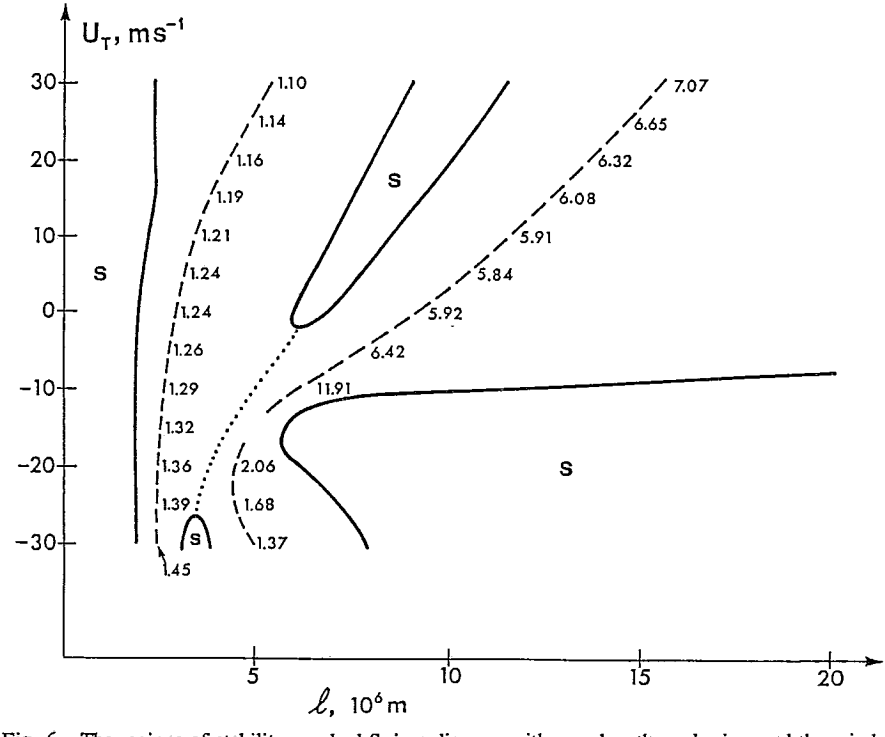

Fig. 6. The regions of stability, marked S, in a diagram with wavelength as abscissa and the windshear in the upper layer U_T as ordinate. The dashed lines are lines of maximum instability, and numbers indicate e-folding times in days. The dotted line gives the curve for minimum instability. Parameters $U_B = 15\ \mathrm{ms}^{-1}$, $\eta_B = \eta_T = 6.5 \cdot 10^{-3}\mathrm{Km}^{-1}$.

and L is sufficiently large. In the regions of instability the dashed lines indicate as in Fig. 1 the curves of minimum e-folding times given in the figure in days. For the short waves we find a decrease in the e-folding time as U_T increases, while the minimum for the long waves is found at $U_T = 5\,\mathrm{ms}^{-1}$ and $L = 10.5 \cdot 10^6\,\mathrm{m}$. The dotted line connecting the two regions of stability is the line of minimum instability.

The structure of the waves varies strongly with the windshear U_T. This can be seen from Fig. 7 in which we have plotted the phase differences for $U_B = 15\,\mathrm{ms}^{-1}$ and $L = 4 \cdot 10^6\mathrm{m}$ as a function of U_T. As long as U_T is large and negative it creates an eastward sloping wave in the upper part of the model while the slope is westward in the lower half of the atmosphere where the wind increases with height. This situation changes when U_T becomes small and negative and for $U_T > 0$ we find the normal westward sloping wave. The amplitude ratios are also shown in Fig. 7. In other words, a growing wave will slope upwind, what ever the direction of the basic flow may be.

Fig. 8 corresponds to Fig. 7, but this time the wavelength is $14 \cdot 10^6\mathrm{m}$, corresponding to wave number 2. Unstable waves exist as we have seen only when $U_T \geq -5\,\mathrm{ms}^{-1}$. They slope westward by a little more than half the wavelength and generally speaking $a_1 > a_5 > 1$.

Among the parameters which may be varied in the steady state we shall now look at the two static stabilities. From many other studies we know that the static stability is

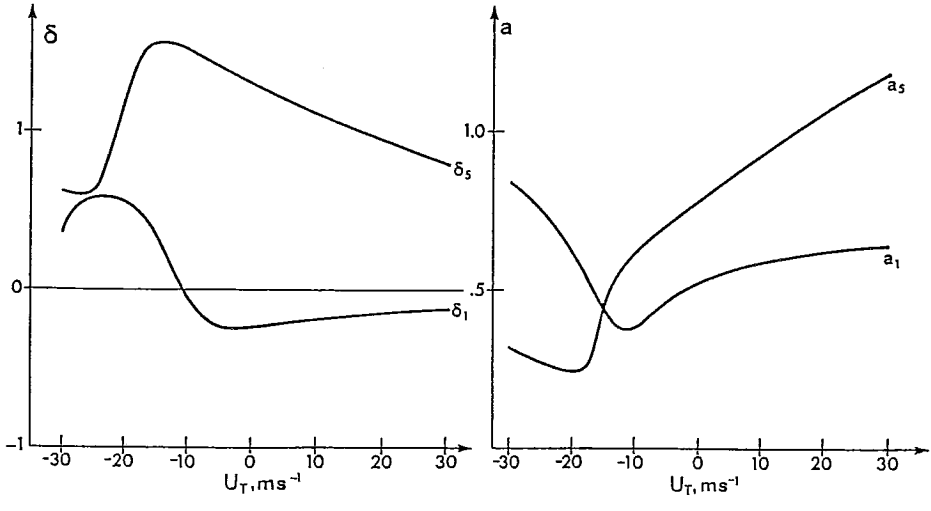

Fig. 7. The relative phases (δ_1 and δ_5) and the relative amplitudes (a_1 and a_5) as a function of U_T. Parameters: $U_B = 15\ \mathrm{ms}^{-1}$, $\eta_B = \eta_T = 6.5 \cdot 10^{-3}\mathrm{Km}^{-1}$, $L = 4 \cdot 10^6\mathrm{m}$.

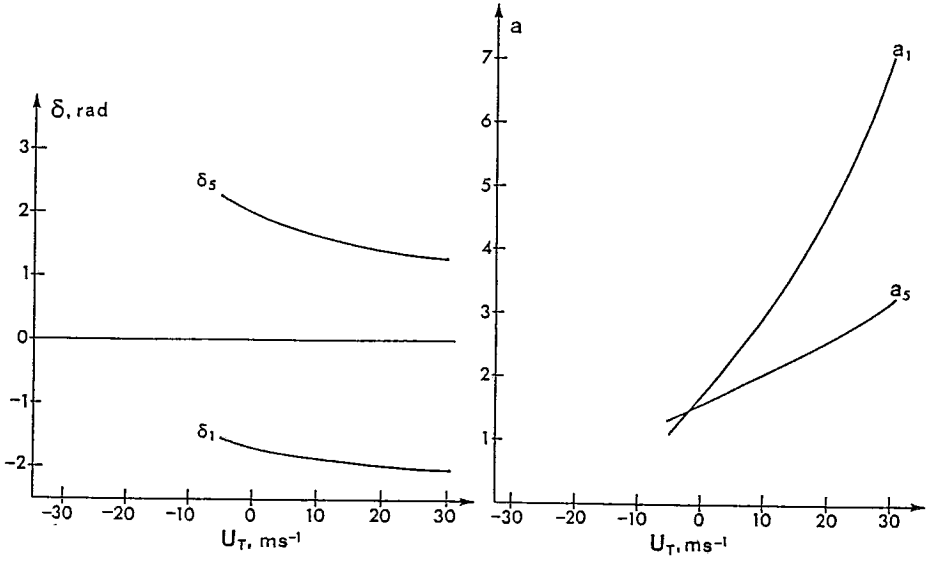

Fig. 8. As Fig. 7, but for $L = 14 \cdot 10^6$m.

responsible for the baroclinic stability usually found for short waves as we have seen also in this study. In other words, the static stability determines the short wave cut-off. As a matter of fact, in the two-level model the short wave stability is determined by the condition

$$L_s = \frac{2\pi}{\sqrt{q^2}} \tag{3.1}$$

where

$$q^2 = \frac{2f_0^2}{\sigma p^2} \qquad (P = 50 \text{ cb}) \tag{3.2}$$

It is thus seen that L will be small if q is large, and this will be the case if σ is small. Adapting (2.5) to the two-level model we may write

$$\sigma = \frac{R^2 T_0}{g p_0^2}(\eta_d - \eta) 2^{\left(2 - \frac{R\eta}{g}\right)} \tag{3.3}$$

For $\eta = 6.5 \cdot 10^{-3}\text{Km}^{-1}$ we find that $\sigma = 2.92$ and thus $L_s = 3.8 \cdot 10^6$m. On the other hand, if $\eta = 9.9 \cdot 10^{-3}\text{Km}^{-1}$ we have $\sigma = 0.0778$ and $L_s = 6.2 \cdot 10^5\text{m} = 620\,\text{km}$. For such a short wave cut-off in the two-level model we would require an almost adiabatic layer which goes through the whole depth of the atmosphere, but this is not the case

for the three level model. In this investigation we shall use the standard placement of the levels, but they may of course be moved as was done by *Wiin-Nielsen* (1989) to investigate the importance of baroclinic instability for the formation of polar lows.

In this paper we shall look only at the stability of a steady state in which a stable layer ($\eta_T = 6.5 \cdot 10^{-3}\mathrm{Km}^{-1}$) is on top of a lower layer with a stratification approaching the adiabatic lapse rate. The corresponding e-folding times are shown in Fig. 9. It is seen that the closer the lapse-rate is to the adiabatic lapse rate the smaller is the wavelength of minimum e-folding time. For values very close to η_d we find maximum growth rates at a wavelength of only a few hundred kilometers. At the same time we find e-folding times which are a small fraction of a day. For details of these cases the reader is referred to *Wiin-Nielsen* (1989).

The instability, discussed above, is apparently not the same instability as the one found by *Moore and Peltier* (1989) in their extensive investigation of stability using the primitive equations. The latter short wave instability appears in models with high vertical resolution or continous vertical stratification.

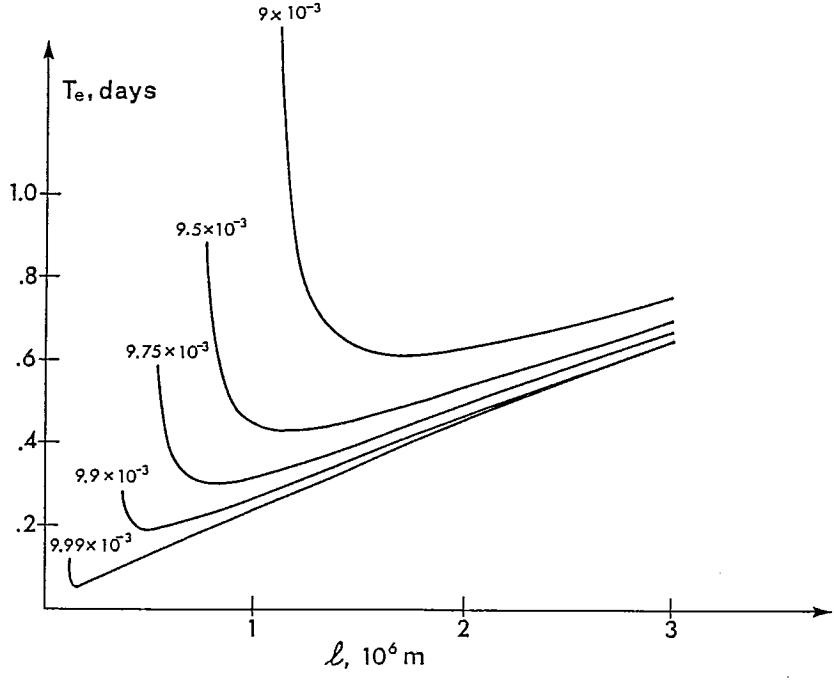

Fig. 9. The e-folding time as a function of wavelength for the following values of η_B: $9 \cdot 10^{-3}$, $9.5 \cdot 10^{-3}$, $9.75 \cdot 10^{-3}$, $9.9 \cdot 10^{-3}$ and $9.99 \cdot 10^{-3}\mathrm{Km}^{-1}$. Other parameters: $\eta_T = 6.5 \cdot 10^{-3}\mathrm{Km}^{-1}$, $U_B = U_T = 15\ \mathrm{ms}^{-1}$.

4. *Concluding remarks*

The present investigation has shown that the three-level, quasi-nondivergent model can have three distinct regions of instability. In addition to the normal region of unstable medium-long waves which occur typically for a normal stratification and a wind increasing with height, and which is present also in a two-level model, there is a weak instability for long waves for some windshears and a strong instability for short waves if one of the two lapse rates approaches the adiabatic lapse rate.

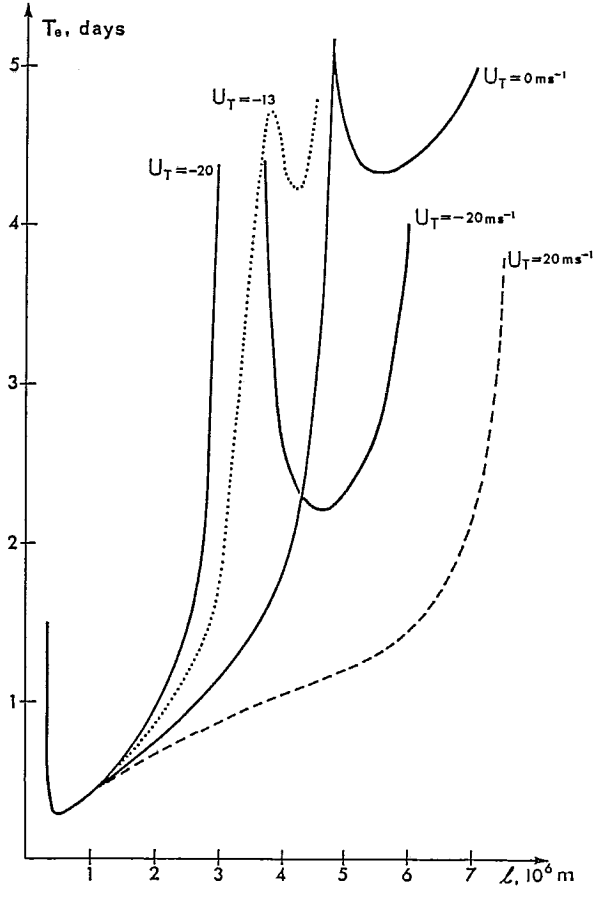

Fig. 10. The *e*-folding time as a function of wavelength for four cases: U_T = -20 ms^{-1} (thin solid line) and U_T = -13 ms^{-1} (dotted line), U_T = 0 ms^{-1} (heavy solid line) and U_T = 15 ms^{-1} (dashed line). Other parameters: U_B = 10 ms^{-1}, $\eta_B = 9.9 \cdot 10^{-3}$Km^{-1} and $\eta_T = 6.5 \cdot 10^{-3}$Km^{-1}.

The two instabilities for medium-long and long waves can be clearly separated in some cases as in Fig. 1, but for some other windshears (see Fig. 7) the two regions are separated only by a region of weaker instability.

The instability for short waves, occurring, say for η_B approaching η_d, goes sometimes over in the instability for medium-long waves in a continuous fashion. It may also happen, as we shall demonstrate, that these regions are clearly separated. An example is given in Fig. 10 showing the e-folding time as a function of wavelength for a case where $U_B = 10\,\mathrm{ms}^{-1}$, $U_T = -20\,\mathrm{ms}^{-1}$, $\eta_B = 9.9 \cdot 10^{-3}\mathrm{Km}^{-1}$, and $\eta_T = 6.5 \cdot 10^{-3}\mathrm{Km}^{-1}$. There is clearly a region of stability between the short wave instability with $T_{e,\min}$ at $L = 500\,\mathrm{km}$ and the medium-long wave instability where T_e is a minimum for $L = 4.6 \cdot 10^6$. If U_T is increased from $-20\,\mathrm{ms}^{-1}$, we find that the two regions join into one at $U_T = -13\,\mathrm{ms}^{-1}$ (see the dotted curve). Such joined regions can be seen also at $U_T = 0$ (second full curve), while the curve for $U_T = 20\,\mathrm{ms}^{-1}$ at most shows a slight change of slope.

Fig. 10 shows clearly that the small scale instability is determined by how close η_B is to η_d, and that this instability is almost independent of U_B and U_T. On the other hand, the medium scale instability as shown by Fig. 6 is present for many combinations of U_T and U_B. Finally, as shown in section 3 the large scale instability exists only when the model contains a vertical variation of the stability parameter $\sigma = \sigma(p)$. However, the instability may be surpressed by large, negative values of U_T as also shown in Fig. 6.

Concerning the vertical slope we find that under normal conditions (i.e. standard lapse rates and the zonal wind increasing with height) the wave slopes to the west. However, the introduction of a negative windshear in a layer will have a tendency to change the slope of the wave in the direction of an eastward slope or a decrease of the westerly slope.

The amplification rate for the long wave instability is so small that this instability is of small importance for practical purposes. The other two instabilities have amplification rates which make them very important in small and medium scale dynamics of the atmosphere.

5. *References*

Charney, J.G., 1947: The dynamics of long waves in a baroclinic, westerly current. *J. Meteor.*, **4**, 135–162.

Cressman, G.P., 1961: A diagnostic study of a midtropospheric development. *Mon. Wea. Rev.*, 89, 74–82.

Eady, E.T., 1949: Long waves and cyclonic waves. *Tellus*, **1**, No. 3, 33–52.

Eliassen, A., 1952: Simplified dynamic models of the atmosphere, designed for the purpose of numerical weather prediction. *Tellus*, **4**, 145–156.

Green, J.S.A., 1960: A problem in baroclinic instability. *Q. J. Roy. Met. Soc.*, 86, 237–251.

Jacobs, S.J. and Wiin-Nielsen, 1966: On the stability of a barotropic basic flow in a stratified atmosphere. *J. Atm. Sci.*, **23**, 682–687.

Moore, G.W.K. and W.R. Peltier, 1989: Nonseparable baroclinic instability, Part I: Quasi-geostrophic dynamics. *J. Atm. Sc.*, **46**, 57–78.

Phillips, N.A., 1954: Energy transformations and meridional circulations associated with simple baroclinic waves in a two-level, quasi-geostrophic model, *Tellus*, **6**, 273–286.

Wiin-Nielsen, A., 1961: Diagnosis of divergence in a three-parameter numerical prediction model. *Mon. Wea. Rev.*, 89, 67–73.

Wiin-Nielsen, A., 1967: On baroclinic instability as a function of the vertical profile of the zonal wind. *Mon. Wea. Rev.*, **95**, 733–739.

Wiin-Nielsen, A., 1989: On the precursors of polar lows, Proc. Conf. on Polar Lows, Madison, Wisconsin, April, 1988